ISBN: 978-3-95450-249-3 ISSN: 2673-5350 doi: 10.18429/JACoW-IBIC2024-WEP04

AN X-RAY PINHOLE CAMERA FOR SESAME STORAGE RING

H. Al-Mohammad, A. Hasoneh, M. Shehab, O. Kailani, SESAME, Allan, Jordan

Abstract

An X-Ray pinhole camera beamline has been installed recently at SESAME storage ring as a very beneficial non-destructive tool, used to characterize the electron beam size and behaviour. The design of the beamline is kept as simple as possible with a modification on the copper absorber to provide a sufficient flux of X-ray proper for imaging. The beamline is under operation now and used for the measurement of beam size, emittance, coupling in the ring, and detection of beam instabilities. This paper describes the design details, simulations and measurement results obtained during the beamline commissioning.

INTRODUCTION

The SESAME Storage Ring (SR) is a 2.5 GeV 133.2 m circumference composed of 8 DBA cells with dispersion in all straight sections (8*4.4 m and 8*2.4 m). It offers a maximum capacity of 25 beamlines, phase 1 current up to 300 mA and Emittance 26 nm.rad [1]. The designed parameters of the storage ring are presented in Table 1.

The X-ray diagnostic beamline was installed and commissioned in the SESAME storage ring in the beginning of 2023. This beamline has been designed to measure the transverse beam profile and emittance and monitor beam stability during the beam decay.

Table 1: Storage Ring Main Parameters

Energy (GeV)	2.5
Circumference (m)	133.2
RF Frequency (MHz)	499.654
Betatron tunes Q_X / Q_Y	7.23 / 6.19
Horizontal emittance ε_x (nm.rad)	26
Momentum compaction factor	0.0083
Circulating Current(mA)	300
Energy loss per turn (keV)	603

PINHOLE CAMERA SETUP

The X-ray pinhole camera consists of a source, a pinhole, a screen, and a camera. At SESAME, the X-ray pinhole camera is installed in cell 16 of the storage ring (SR) to measure the beam size from the 6.5° port of the bending magnet (BM). The X-ray beam passes through a beam port absorber, which is a copper block designed to absorb the majority of the X-ray beam while allowing a portion of the high-energy X-rays to pass through to the pinhole assembly in air, and subsequently to the YAG screen and imaging system. The system layout is illustrated in Fig. 1. The pinhole assembly should be positioned as close to the source as possible to achieve greater magnification; in our setup, it is located 3.5 meters away. The pinhole is created using 1 mm thick tungsten bars separated by chemically etched shims, with four layers of shims (10, 25, 50, and 400μm) forming a grid [2]. To image the source, a fluorescent screen, which absorbs X-rays and fluoresces in the visible spectrum, is used. This screen is placed 5.3 meters away from the pinhole assembly, resulting in an image magnified by a factor of approximately 1.5. A CCD camera with a zoom lens is employed to capture and measure the size of the source.

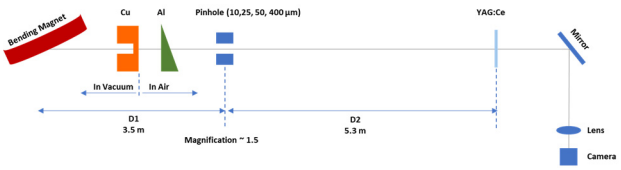

Figure 1: Layout of X-ray pinhole camera beamline.

X-Ray Beam Absorber

The X-ray beam absorber was originally designed to be made of copper, featuring a slot for a port leading to an aluminium window. However, due to financial constraints, an alternative approach was adopted. The solution involved repurposing a defective full copper mirror, previously used in the diagnostics beamline in the storage ring, designed to handle an X-ray beam of 400 mA at 2.5 GeV.

To repurpose the mirror as an absorber and beam extractor with minimal absorption in its thin layer that will extract part of the beam after polishing its surface, simulations and finite element analysis (FEA) were conducted. The primary challenge was drilling the mirror and offsetting the hole from the centre to avoid damaging the cooling channels, one of them is located at the centre. This offset was then compensated by precisely aligning the entire absorber (mirror) chamber.

The absorber is expected to receive a maximum normal peak power of 26.08 W/mm² from the dipole magnet at 300 mA. FEA results indicate that the maximum temperature will reach 84.8°C, with a maximum Von Mises stress of 146 MPa. A 3 mm circular slot was drilled from the inner face and a 6 mm slot from the outer face of the mirror, leaving a 0.5 mm thick layer of copper to allow the beam to pass through while maintaining vacuum integrity, as illustrated in Fig. 2. The 0.5 mm thickness was chosen to provide an adequate amount of flux while meeting mechanical requirements and ensuring the feasibility of in-house fabrication. As a consequence of using copper instead of aluminium the intensity of the final beam is significantly reduced, as illustrated in Fig. 3, and the electron beam at injection energy (800MeV) can't be seen or measured. The beam is started to be seen at ~ 2.4 GeV, and the photon intensity at 2.5 GeV keeps sufficient to see the beam over the decay time in the SR. The aluminium wedge was ultimately not used due to the reduced photon intensity. The copper absorber shifted the X-ray beam energy to be

ISBN: 978-3-95450-249-3 ISSN: 2673-5350 doi: 10.18429/JACoW-IBIC2024-WEP04

~38 keV, as given by the simulation of the overall system done on SHADOW and XOP in OASYS software [3].

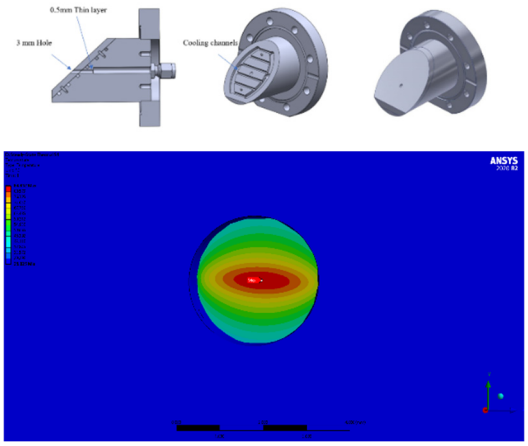

Figure 2: Defected mirror used as absorber, left 2D side view, middle the internal face with cooling channels and right the 3D view (up), the thermal distribution of the 3mm diameter 0.5 mm thick copper layer.

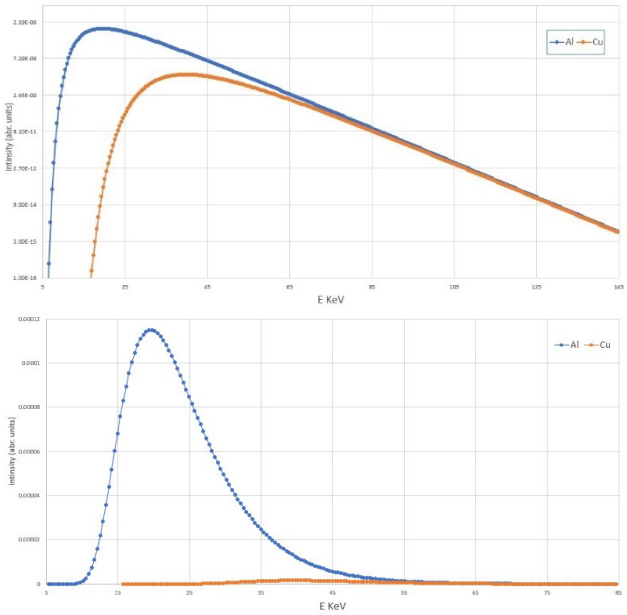

Figure 3: Spectrum of extracted X-ray photon beam showing how copper attenuate the intensity and shift the energy in logarithmic scale (up) linear (down).

Pinhole Assembly and Optical System

The pinhole assembly is composed of Tungsten bars stacking two orthogonal sets of (25 mm ×1 mm ×5 mm) tungsten blades separated by precisely machined shims as built at Diamond Light Source [4], The four layers of shims create 16 pinholes with sizes of 10, 25, 50, and 400 µm. The assembly is mounted on a motorized stage with five degrees of freedom and micro-stepping capability, allowing for highly precise remote alignment and scanning of the pinholes.

The imaging system consists of a YAG:Ce screen with a thickness of 200 µm, which converts X-rays into visible light. This scintillator is well-suited for imaging with lower energy levels and provides strong emission at the higher energies used in our setup. Following the screen, a fused silica mirror is mounted at a 45° angle, directing the light to a zoom lens that focuses the beam onto a CCD camera. The camera is positioned below the radiation plane and shielded with lead to protect it from radiation damage, particularly since it is located in the injection area.

The 2D Gaussian method is utilized to fit and calculate the beam size using Python. To ensure precise results, the exposure time is carefully adjusted (up to 300 ms) to maintain the image's maximum intensity without affecting the calculation outcomes or causing saturation, while keeping the gain low and fixed. This approach allows for the use of a single gain curve and minimizes noise amplification.

PSF OF PINHOLE CAMERA

The image formed on the camera is the convolution of the source profile, and of the point spread function (PSF) of the diffraction through the pinhole, and of the PSF of the X-ray camera. The total PSF contribution is composed quadratically to the total resolution of the X-ray pinhole camera and approximated to be Gaussian PSF [5] overall PSF may be represented as:

$$\sigma_{PSF}^2 = \sigma_{pinhole}^2 + \sigma_{image}^2 \quad (1)$$

The PSF contribution associated with imaging the scintillator screen, lens and camera denoted by σ_{image} may be measured using a knife-edge method or by sector star.

Pinhole PFS can be derived analytically by calculating two contributions, diffraction through the pinhole and geometrical contribution due to the finite size of the pinhole which are described by the equation below:

$$\sigma_{pinhole}^2 = \sigma_{diffraction}^2 + \sigma_{aperture}^2 \quad (2)$$

$$\sigma_{diffraction}^2 = \frac{\sqrt{12}}{4\pi}\frac{\lambda D}{A} \quad (3)$$

$$\sigma_{aperture}^2 = \frac{A}{\sqrt{12}}\frac{D+d}{d} \quad (4)$$

Where d is the distance from source to pinhole and D pinhole to screen, λ is the wavelength, and A the pinhole aperture. To calculate the optimum working point for the pinhole, we evaluate the point spread function (PSF) by varying the aperture size from 5µm to 50µm, but using only one thickness (without any attenuation) due to intensity limitations caused by the Cu window. Figure 4 illustrates the PSF as a function of pinhole size at two different energies: 18 keV for a 1 mm Al window, which corresponds to the original absorber design, and 38 keV for the current setup with a 0.5 mm Cu window. The optimum aperture that minimizes the PSF is:

ISBN: 978-3-95450-249-3 ISSN: 2673-5350 doi: 10.18429/JACoW-IBIC2024-WEP04

$$A^2_{Optimum} = \frac{12}{4\pi}\frac{\lambda dD}{d+D} \quad (5)$$

The calculations and simulation show that the best pinhole size for min. PSF with respect to intensity is (25×25 μm^2).

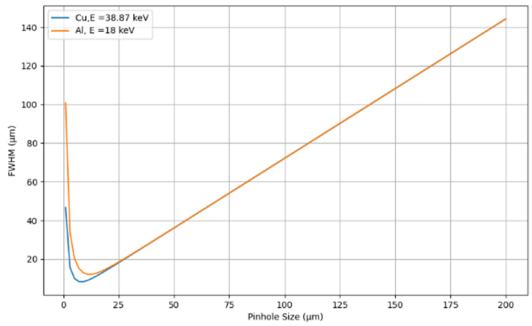

Figure 4: FWHM of the PSF from Pinhole as function of different apertures for 1mm Al (18 keV) and 0.5mm Cu (38 keV) windows.

MEASURMENTS RESULTS

Measurements of the emittance can be done indirectly by measuring the transverse beam size using the synchrotron radiation produced by it. The horizontal and the vertical emittance are calculated by using the following formula:

$$\sigma_i^2 = \beta_i \varepsilon_i + (\eta_i\, \sigma_\varepsilon)^2, \quad (6)$$

where σ_i is the measured beam size in the horizontal or vertical plane, respectively ($i = x, y$), β_i and η_i are the betatron and dispersion functions at the source point and in the corresponding plane, ϵ_i and σ_ε are the emittance and the relative energy spread of the electron beam.

The parameters β_x, η_x and σ_ε are known from the model and the data given by the linear optics measurements and optimisation procedure known as LOCO. The dispersion can be measured by varying the storage ring RF frequency by 100 Hz and calculate the slope of the linear displacement of the centroid of the electron beam measured by the pinhole images [6].

In the vertical plane the dispersion is assumed to be zero. The beam sizes, for corrected optics, are measured as shown in Fig. 5.

The results from both planes show strong agreement with the machine's design. The coupling was measured locally at the pinhole location, providing values that are relatively consistent with the global coupling measured using the closest tune method. The measured emittance values closely match the machine's design specifications, with 26 nm.rad for the horizontal plane and 0.25 nm.rad for the vertical plane.

The stability of the measurement is in good shape since the machine works in decay mode with single injection a day, where the beam decays from 250 mA to ~130 mA. Although the intensity is reduced with the decay nevertheless, we stay on same gain and exposure time of the camera. Figure 6 shows the stability achieved over 24 hours for both planes.

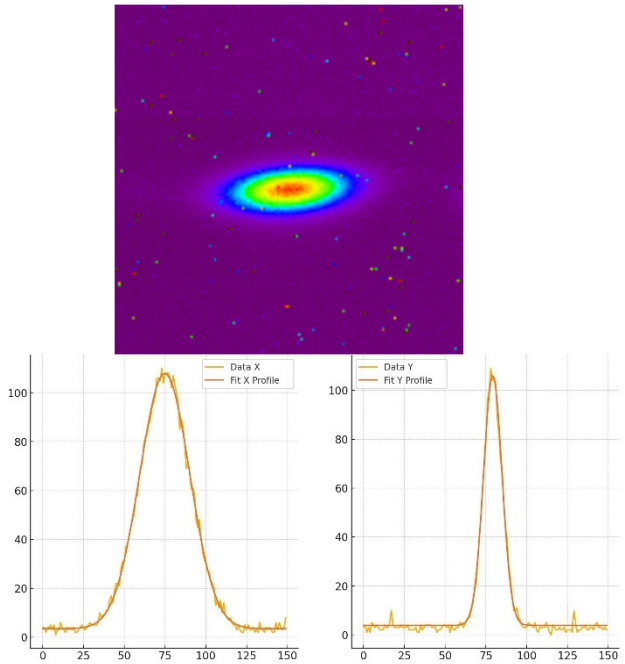

Figure 5: Beam image from the pinhole camera and fitted profiles, using 2D Gaussian fit, for horizontal (left) and vertical (right) beam sizes.

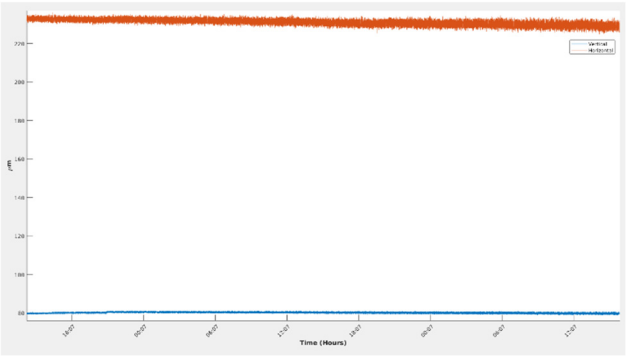

Figure 6: Stability of beam size measurement for 24 hours, the orange is horizontal with a drifting around 2μm and blue is vertical with drifting less than 1 μm with decay beam.

CONCLUSION

This paper presents the design of the pinhole camera for SESAME SR. The successful installation and commissioning of the X-ray pinhole camera allows now to measure the emittance, helps to monitor bunch instabilities and avoid transverse emittance blow-up by tracking beam size behaviour.

ACKNOWLEDGEMENTS

The authors would like to thank everyone who contributed to this design and installation through discussions and suggestions. Special appreciation and thanks to G. Rehm from BESSY and L. Bobb from Diamond for their support, help and the valuable discussions.

ISBN: 978-3-95450-249-3 ISSN: 2673-5350 doi: 10.18429/JACoW-IBIC2024-WEP04

REFERENCES

[1] M. Attal *et al.*, "Commissioning of SESAME Storage Ring", in *Proc. IPAC'17*, Copenhagen, Denmark, May 2017, pp. 2694-2696. doi:10.18429/JACoW-IPAC2017-WEPAB050

[2] P. Elleaume, C. Fortgang, C. Penel and E. Tarazona, "Measuring Beam Sizes and Ultra-Small Electron Emittances Using an X-ray Pinhole Camera", *J. Synchrotron Radiat.*, vol. 2, p. 209, 1995. doi:10.1107/S0909049595008685

[3] https://www.aps.anl.gov/Science/Scientific-Software/OASYS

[4] L. M. Bobb, A. F. D. Morgan, and G. Rehm, "Performance Evaluation of Molybdenum Blades in an X-ray Pinhole Camera", in *Proc. IBIC'16*, Barcelona, Spain, Sep. 2016, pp. 795-798. doi:10.18429/JACoW-IBIC2016-WEPG63

[5] Cyrille Thomas, Guenther Rehm, Ian Martin and Riccardo Bartolini "X-ray pinhole camera resolution and emittance measurement", *Phys. Rev. ST Accel. Beams*, vol.13, Feb. 2010, p. 022805. doi:10.1103/PhysRevSTAB.13.022805

[6] C. A. Thomas and G. Rehm, "Pinhole Camera Resolution and Emittance Measurement", in *Proc. EPAC'08*, Genoa, Italy, Jun. 2008, paper TUPC086, pp. 1254-1256.